Journal of Quantitative Spectroscopy & Radiative Transfer 94 (2005) 273–290

Journal of Quantitative Spectroscopy & Radiative Transfer

www.elsevier.com/locate/jqsrt

Light reflection and transmission by multi-layered turbid media

A.A. Kokhanovsky[a,b,*], V.V. Rozanov[a]

[a]Institute of Environmental Physics, University of Bremen, FB 1, P.O. Box 330440, Otto Hahn Allee 1, Kurfsteiner Strasse 1, 28334 Bremen, Germany
[b]Institute of Physics, 70 Skarina Avenue, Minsk 220072, Belarus

Received 16 March 2004; accepted 12 September 2004

Abstract

This paper is devoted to the derivation of simple approximate equations for transmission and reflection functions of multi-layered disperse media. It is assumed that each layer is optically thick and weakly absorbing. Equations obtained can be used in various fields of applied optics, including cloud and snow optics.

Keywords: Multiple light scattering; Multi-layered turbid media; Clouds; Radiative transfer; Reflection; Transmission

1. Introduction

Vertically inhomogeneous disperse media are of a frequent occurrence both in nature (e.g., multi-level cloud systems, snow deposited at different times at a given place, terrestrial atmosphere and ocean, biological tissues, etc.) and technological applications (multi-layered painted surfaces, paper, etc.). This explains a great interest in studies of radiative transfer in vertically inhomogeneous media. Recent advances in this area have been summarized by

*Corresponding author. Institute of Environmental Physics, University of Bremen, FB 1, P.O. Box 330440, Otto Hahn Allee 1, 28334 Bremen, Germany. Tel.: +49 421 218 4475; fax: +49 421 218 4555.
E-mail address: alexk@iup.physik.uni-bremen.de (A.A. Kokhanovsky).

doi:10.1016/j.jqsrt.2004.09.011

Yanovitskij [1]. A great number of exact (see, e.g., [2,3]) and approximate [2,4–7] techniques has been developed. At present time there is no problem to account for an arbitrary vertical inhomogeneity of a horizontally homogeneous plane-parallel light scattering medium. However, it appears that for this, one needs to perform quite complex numerical calculations with the use of up-to-date computer technology. On the other hand, the practical work requires simple approximate solutions, which can be used to perform rapid estimations of the influence of vertical inhomogeneity on light reflection and transmission by turbid media. With this in mind, we have decided to derive such approximations based on our recent work for a single homogeneous optically thick disperse layer [8] and also on earlier works of Rozenberg [9], Melnikova and Minin [10], and Zege et al. [11]. To derive approximate solutions, we make an assumption that the probability of light absorption by particles in a disperse medium is close to zero (smaller than approximately 3%).

2. Theory

2.1. Reflection

Let us assume that a disperse medium is composed of several light scattering layers having different light scattering characteristics (e.g., the phase function $p(\theta)$, the absorption σ_{abs} and extinction σ_{ext} coefficients). The geometry of the problem is shown in Fig. 1. Light enters a disperse medium at the angle θ_0. The reflected light is observed at the angle θ_1 and the diffusely transmitted light is observed in the direction specified by the angle θ_2. We need to model the intensity of diffusely reflected and transmitted beams taking into account effects of vertical inhomogeneity of the medium under consideration.

Note that we put no limitations on the number of layers in a disperse medium. In Fig. 1 we show a situation, which can be a case in the terrestrial atmosphere with several cloud layers at different heights. Then the height in Fig. 1 is given in kilometers. So we refer to these layers as clouds in this paper. Although layers can be composed of other disperse substances and materials, the region which separates clouds is assumed to be free of light scattering and absorption. In particular, it means that the situation we consider is equivalent to the touching light scattering layers (e.g., several snow layers). This assumption, however, is not crucial for the theory developed here (e.g., absorption and scattering of light by gases and aerosols between clouds can be accounted for, if needed (see, e.g. [8])). We assume that all layers are optically thick ($L_i \gg l_i$, where L_i is the geometrical thickness of i-layer and l_i is the photon free path length in the layer, which is equal to the inverse value of the extinction coefficient in a given layer) and weakly absorbing (the probability of photon absorption $\beta = \sigma_{\mathrm{abs}}/\sigma_{\mathrm{ext}} \to 0$). We need these assumptions to apply the modified asymptotic theory for each layer as specified by Kokhanovsky and Rozanov [8] (see Appendix A). There are no limitations on the type of the phase function, however. Although our assumptions severely restrict the applicability of the model to many real-world media, they do provide an accurate approach to the solution of a number of important problems (e.g., in optics of clouds, snow, biological tissues and paints).

The starting point is the expression for the reflection function of a single homogeneous optically thick weakly absorbing layer. It can be written in the following form for a scattering layer above a

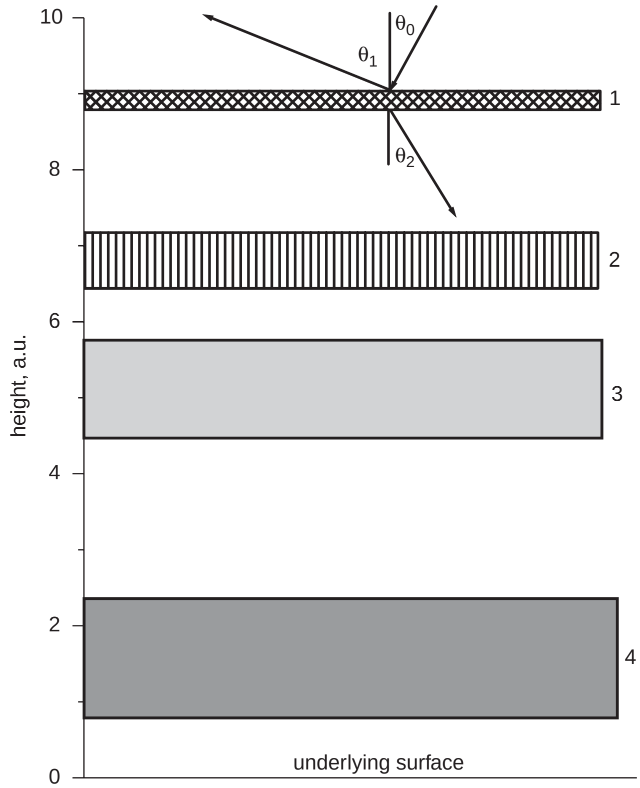

Fig. 1. The geometry of the problem.

Lambertian surface with the albedo A [12]:

$$R_A(\xi,\eta,\tau) = R(\xi,\eta,\tau) + \frac{At_{\mathrm{d}}(\xi)t_{\mathrm{d}}(\eta)}{1-Ar}. \tag{1}$$

Here (see Appendix A)

$$R(\xi,\eta,\tau) = R_\infty(\xi,\eta) - T(\xi,\eta,\tau)\exp(-x-y) \tag{2}$$

is the reflection function of a scattering layer for the black ($A=0$) underlying surface, $R_A(\xi,\eta,\tau)$ is the same function but for the scattering layer–underlying surface system, $x = k\tau$, $k = \sqrt{3\beta(1-g)}$ is the diffusion exponent, g is the asymmetry parameter, which is easily obtained by the integration of the phase function with respect to scattering angle [13], $\tau = \sigma_{\mathrm{ext}}l$ is the optical thickness, l is the geometrical thickness of a scattering layer, $y = 4k/3(1-g)$, r is the spherical albedo of a scattering layer for an illumination from below at $A=0$, $t_{\mathrm{d}}(\xi)$ is the diffused transmittance for the illumination in the direction $\theta_0 = \cos^{-1}(\xi)$ (see Fig. 1), $T(\xi,\eta,\tau)$ is the transmission function at $A=0$. The function $t_{\mathrm{d}}(\eta)$ is the diffused transmittance for the illumination in the direction $\theta_2 = \cos^{-1}(\eta)$. The dependence of the reflection function in Eq. (1) on the azimuth ϕ is omitted for simplicity. Also we neglect the direct light transmittance, which takes rather small values for optically thick layers. Convenient approximate equations for functions $T(\xi,\eta,\tau)$, $t_{\mathrm{d}}(\xi)$, $R_\infty(\xi,\eta)$ and r are given in Appendix A (see also ref. [13]).

Let us proceed further now. It is known that the reflection of light from an optically thick weakly absorbing strongly light scattering layer is rather close to that of a Lambertian reflector. This is due to well-developed multiple light scattering in the medium in this case. Therefore, to find the reflectance from a multi-layered system as given in Fig. 1, we propose to use Eq. (1) with A substituted by the spherical albedo r_2^* of the multi-layered system below the upper layer (see Fig. 1). Other functions in Eq. (1) then refer to the first layer from the illumination side. Such an approach was proposed and successfully used by Melnikova and Minin [10] for studies of light fluxes in a cloudy atmosphere.

The spherical albedo r_2^* can be easily found integrating Eq. (1). Indeed, it follows from Eq. (1) (see Appendix A):

$$r_2^* = r_2 + \frac{t_2^2 r_3^*}{1 - r_2 r_3^*}. \tag{3}$$

Here r_3^* is the spherical albedo of the system starting from the third layer down (see Fig. 1), t_2 is the global transmittance of the second layer (see Appendix A for the definition), r_2 is the spherical albedo of the second scattering layer for an illumination from below. The spherical albedo r_3^* can be found using an equation similar to Eq. (3)

$$r_3^* = r_3 + \frac{t_3^2 r_4^*}{1 - r_3 r_4^*} \tag{4}$$

with meaning of all parameters similar to those in Eq. (3). Clearly, we need to repeat this procedure till the underlying surface is reached. Then we have

$$r_n^* = r_n + \frac{t_n^2 A}{1 - r_n A} \tag{5}$$

and the procedure is complete.

Let us check the accuracy of the straightforward procedure outlined above using the exact solution of the radiative transfer equation with SCIATRAN [3] for a two-layered disperse system over a black surface. Then A in Eq. (1) should be substituted by the spherical albedo of a lower layer r_2. All other parameters in Eq. (1) refer to an upper layer. Note that SCIATRAN is a well-documented and thoroughly tested radiative transfer code based on the discrete ordinates approach. Its accuracy is better than 1%.

The results of comparisons are shown in Figs. 2a–c. In particular, we give the dependence of the reflection function of a disperse medium on the incidence angle for the nadir observation. Due to the reciprocity principle, our calculations are also valid for the nadir illumination and varying observation angles.

The middle curves in Figs. 2a–c correspond to a two-layered cloud system with the optical thickness of the bottom layer $\tau_b = 30$ and the optical thickness of the upper layer $\tau_u = 10$. We assume that the upper layer does not absorb incident radiation. The single scattering albedo of the bottom layer is equal to 0.9945 (Fig. 2a), 0.9982 (Fig. 2b) and 0.9681 (Fig. 2c).

The upper curves in the same figure correspond to a single layer having optical thickness $\tau = \tau_b + \tau_u$ and the single scattering albedo equal to 1. Lower curves in Figs. 2a–c correspond to a single layer having optical thickness $\tau = \tau_b + \tau_u$ and the single scattering albedo equal to 0.9945

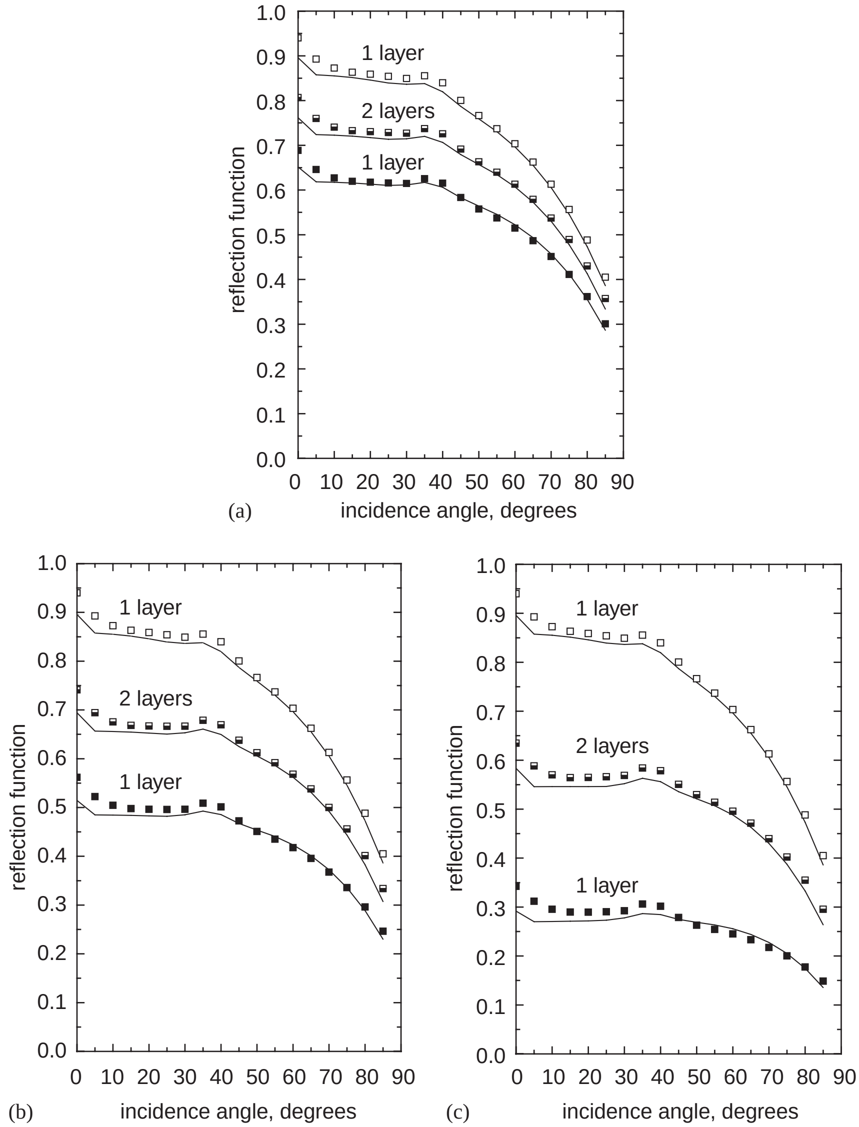

Fig. 2. (a) The dependence of the reflection function of a cloud medium on the incidence angle for the nadir observation. Symbols give exact results and lines are due to the approximation (see details in text). The curve in the middle was obtained for an upper nonabsorbing layer and the absorbing layer with $\omega_0 = 0.9945$ at the bottom. Upper curves correspond to a nonabsorbing single layer. Lower curves correspond to an absorbing single layer. The total optical thickness is kept constant for all calculations ($\tau = 40$). (b) The same as in (a) except $\omega_0 = 0.9892$. (c) The same as in (a) except $\omega_0 = 0.9691$.

(Fig. 2a), 0.9982 (Fig. 2b) and 0.9681 (Fig. 2c). Exact results are shown by symbols. Lines correspond to calculations according to the approximation developed here.

The phase function was found using the narrow gamma droplet size distribution [13] with the effective radius 10 μm and the effective variance equal to $\frac{1}{9}$ at the wavelength $\lambda = 0.65\,\mu$m for

water droplets with the refractive index m equal to $1.331 - 0i$ (Figs. 2a–c, upper curves), $1.331 - 0.00005i$ (Fig. 2a, lower curves), $1.331 - 0.0001i$ (Fig. 2b, lower curves), $1.331 - 0.0003i$ (Fig. 2c, lower curves).

Note that the variation of the imaginary part of the refractive index allows us to model various levels of cloud pollution (e.g., due to black carbon). The phase function differs not significantly for all layers. For instance, the asymmetry parameter equal to 0.85 at $m = 1.331 - 0i$, 0.8513 at $m = 1.331 - 0.00005i$, 0.8525 at $m = 1.331 - 0.0001i$, and 0.8571 at $m = 1.331 - 0.0003i$. This is according to the general fact that the phase function of weakly absorbing particles is not particularly effected by the level of light absorption. However, note that there is a slight tendency for the general increase of the asymmetry parameter with the imaginary part of the refractive index.

It follows from Figs. 2a–c and 3 that the accuracy of our simple approximation is quite high for the case considered. In fact it is comparable with the accuracy of correspondent equations for a single layer or even higher than that (e.g., see Fig. 3 for a single layer at $\omega_0 = 0.9691$). This

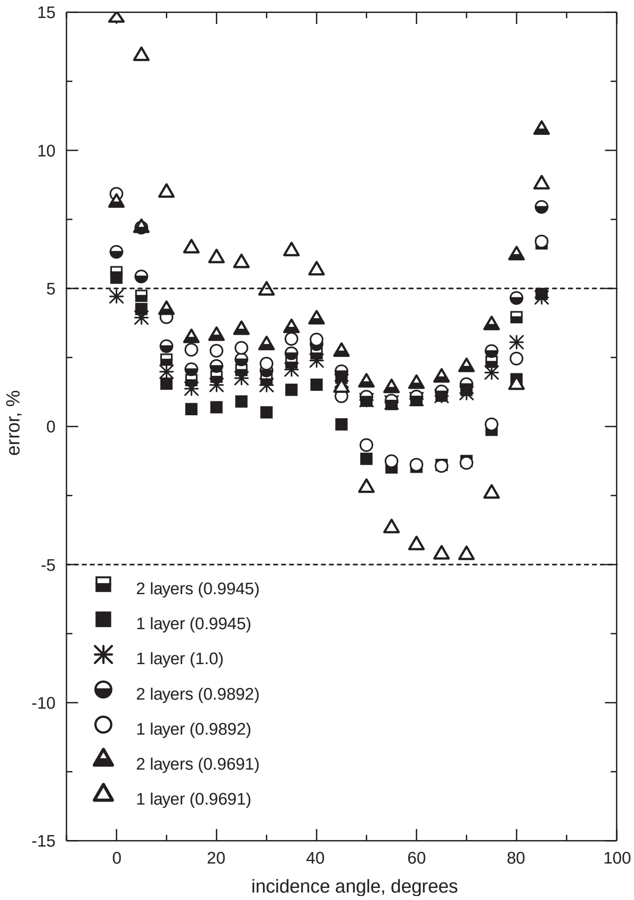

Fig. 3. The relative errors $\delta = 1 - R_a/R_e$ (in percent) for calculations shown in Fig. 2. Here indices a and e signify approximate and exact results, respectively.

paradox is explained by the fact that the accuracy of the approximation is highly influenced by the value of ω_0. The average value of ω_0 is, however, lower for a two-layered system (with a nonabsorbing upper layer) as compared to a single absorbing layer having the same optical thickness.

We see that the two-layered system with the total optical thickness 40 has values of R intermediate between those for an upper layer (at $\tau = 40$) and lower layer (also at $\tau = 40$). This can be expected on general grounds as well. Errors are generally below 5% but they increase for oblique incidence angles. The accuracy decreases with β. The value of $\beta \approx 0.03$ can be considered as an upper boundary for the application of this theory. Although it can be applied to slightly larger values of β if the accuracy is not a primary concern (e.g., for rapid estimations of vertical inhomogeneity effects).

It is interesting to see the performance of equations for larger and smaller values of τ_b, τ_u. This is shown in Figs. 4 and 5 for an absorbing lower layer and nonabsorbing upper layer. We see that the accuracy of our equations is robust against change of the turbid layer thickness. Note that the variation of the optical thickness of a lower layer (see Fig. 4a) does not change the reflection function very much. This is due to the fact that the spherical albedo of a lower absorbing cloud does not depend strongly on τ_b. On the other hand, the variation of the upper layer optical thickness τ_u (see Fig. 5a) changes the result considerably. Cloud becomes much brighter for the larger thickness of the upper layer. Obviously, for a very thick upper layer the sensitivity of the reflection function to the presence of a turbid layer at the bottom is lost. This is similar to the effect of the disappearance of objects in a heavy fog. Therefore, we conclude that high

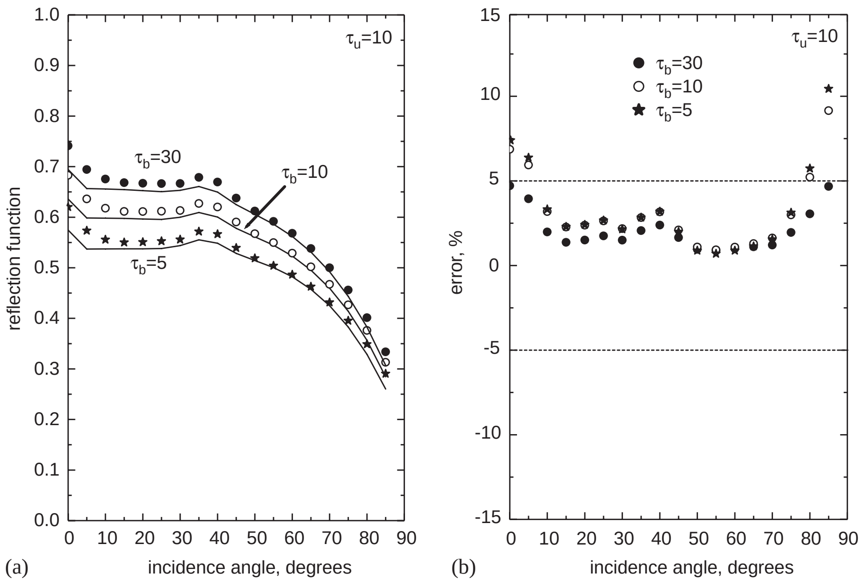

Fig. 4. (a) The dependence of the reflection function of a two-layered cloud medium on the incidence angle for the nadir observation at $\tau_u = 10$ and $\tau_b = 5$, 10, 30. The upper layer does not absorb radiation. The bottom layer is characterized by the single scattering albedo 0.9892 (see Fig. 1b). Symbols give exact results and lines are due to the approximation (see details in text). (b) The relative errors $\delta = 1 - R_a/R_e$ for calculations shown in (a).

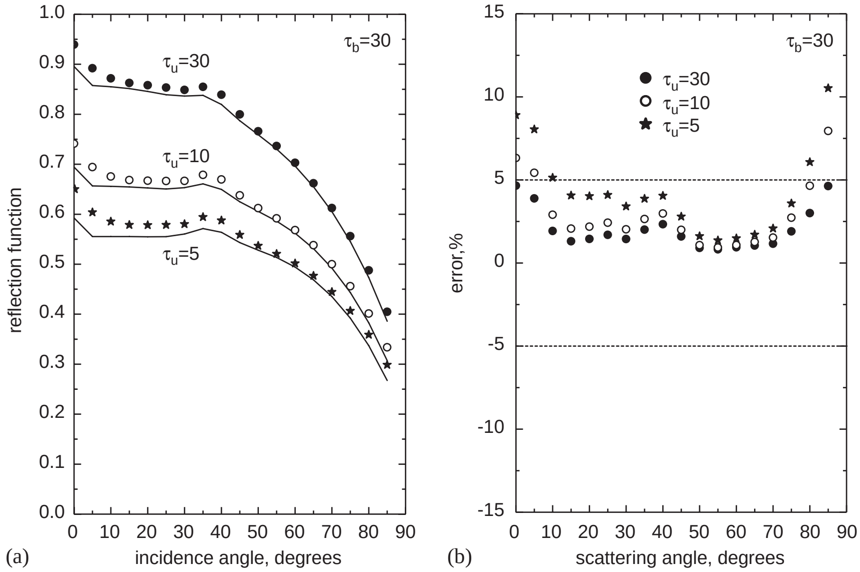

Fig. 5. (a) The dependence of the reflection function of a two-layered cloud medium on the incidence angle for the nadir observation at $\tau_u = 5$, 10, 30 and $\tau_b = 30$. The upper layer does not absorb radiation. The bottom layer is characterized by the single scattering albedo 0.9892 (see Fig. 1b). Symbols give exact results and lines are due to the approximation (see details in text). (b) The relative errors $\delta = 1 - R_a/R_e$ for calculations shown in (a).

nonabsorbing clouds can shield lower (and possibly) polluted clouds. This can lead to important climatic effects not accounted in Global Circulation Models at the moment.

To make this point more clear we present the reflection function of a single absorbing cloud layer with the optical thickness 30 in Fig. 6. Then we add a nonabsorbing cloud at the higher level in the atmosphere. It follows that the reflection of the system considerably increases both for warm water and cold ice upper-level clouds. The phase function of an ice cloud was taken from study of Mishchenko et al. [14] (the fractal particle model) and the phase function of the water cloud was calculated as indicated above (at $m = 1.331 - 0.0001i$ for a lower cloud and $m = 1.331$ for an upper cloud in the two-layered system). The increase in the reflection is much more pronounced for crystalline clouds. It means that ice clouds not only warm the system by trapping terrestrial radiation. They also may shield lower polluted cloud systems (e.g., in urban areas) and increase general reflection of the surface–atmosphere system. This indicates the complexity of the issue of cloud's influence on climate.

2.2. Transmission

The question arises if the model presented above can be applied to studies of light transmission. The answer to this question is positive. Indeed, we have for the transmission function of a single homogeneous disperse layer over a Lambertian surface [12]

$$T_A(\xi, \eta, \tau) = T(\xi, \eta, \tau) + \frac{At_d(\xi)\Re(\eta)}{1 - Ar}. \tag{6}$$

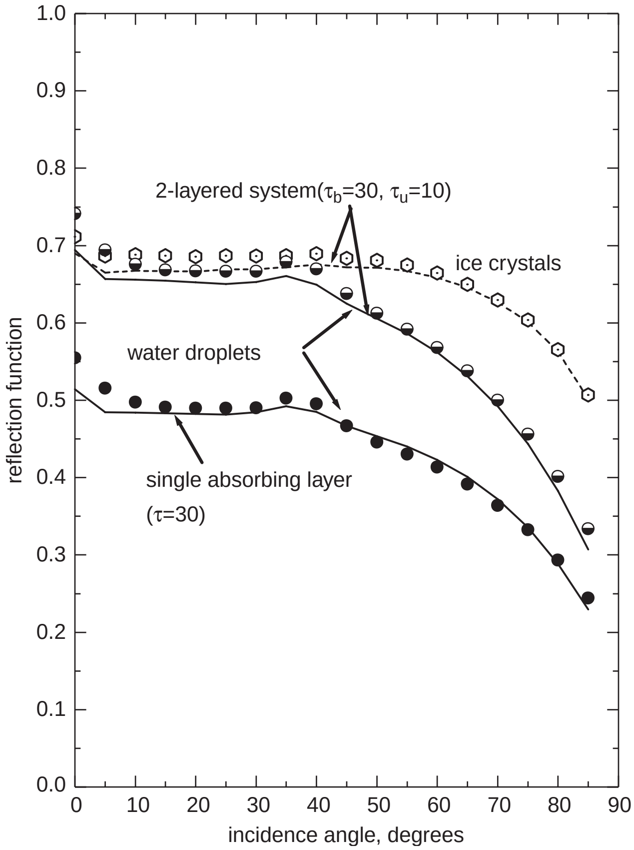

Fig. 6. The dependence of the reflection function on the incidence angle for the nadir observation for a two-layered cloud medium at $\tau_u = 10$, $\tau_b = 30$ (upper curves) and for an absorbing single cloud layer with $\tau = 30$ (lower curves). The upper layer does not absorb radiation and is composed either of water droplets or ice crystals. The bottom layer and a single absorbing layer is characterized by the single scattering albedo 0.9892 (see Fig. 1b). Symbols give exact results and lines are due to the approximation (see details in text).

Here all functions are defined as in Eqs. (1) and (2) and in addition $\Re(\eta)$ is the plane albedo of the layer for the illumination from below (see Appendix A). Again assuming that the layers below the upper one can be substituted by a Lambertian reflector, we have for the transmission function $\bar{T}_1(\xi, \eta)$ of the first layer in the n-layer system

$$\bar{T}_1(\xi, \eta) = T_1(\xi, \eta) + \frac{t_{d1}(\xi)\Re_1(\eta) r_2^*}{1 - r_1 r_2^*}, \tag{7}$$

where we omitted the dependence on the optical thickness and r_2^* is found using the iterative procedure starting from the ground surface as underlined in the previous section. Functions $T_1(\xi, \eta)$, $t_{d1}(\xi)$, r_1 and $\Re_1(\eta)$ have the same meaning as in Eq. (6) but for the first layer.

Let us consider now the transmittance under the second layer. The second layer is illuminated by the diffused light transmitted by the first layer. It follows from Eq. (7) that the diffused

transmittance $\bar{t}_{\mathrm{d}1}(\xi)$ (see Appendix A) is given by

$$\bar{t}_{\mathrm{d}1}(\xi) = t_{\mathrm{d}1}(\xi) + \frac{t_{\mathrm{d}1}(\xi) r_1 r_2^*}{1 - r_1 r_2^*} \tag{8}$$

or

$$\bar{t}_{\mathrm{d}1}(\xi) = \frac{t_{d1}(\xi)}{1 - r_1 r_2^*}. \tag{9}$$

Also we have for the global transmittance from Eq. (9) (see Appendix A)

$$\bar{t}_1 = \frac{t_1}{1 - r_1 r_2^*}. \tag{10}$$

Therefore, the transmission function $\bar{T}_2$ after the second layer in the n-layered system is given as

$$\bar{T}_2(\xi, \eta) = \bar{t}_{\mathrm{d}1}(\xi) \bar{t}_{\mathrm{d}2}(\eta), \tag{11}$$

where (see Eq. (9))

$$\bar{t}_{\mathrm{d}2}(\eta) = \frac{t_{\mathrm{d}2}(\eta)}{1 - r_2 r_3^*}. \tag{12}$$

Following this procedure, we can obtain the transmission function under the third layer

$$\bar{T}_3(\xi, \eta) = \bar{t}_{\mathrm{d}1}(\xi) \bar{t}_2 \bar{t}_{\mathrm{d}3}(\eta), \tag{13}$$

where $\bar{t}_2 = t_2/(1 - r_2 r_3^*)$ and we accounted for the fact that the second layer is illuminated from above by diffused light and it also serves as a diffuse light source for the third layer. Repeating this procedure for each layer, we can arrive finally to the transmission function of a whole system

$$\bar{T}_n(\xi, \eta) = \bar{t}_{\mathrm{d}1}(\xi) \bar{t}_2 \bar{t}_3 \ldots \bar{t}_{n-1} \bar{t}_{\mathrm{d}n}(\eta), \tag{14}$$

where $\bar{t}_j = t_j/(1 - r_j r_{j+1}^*)$ and $r_{n+1} \equiv A$. Interestingly, Eq. (14) can be written in the form similar to that for a homogeneous layer (see Appendix A)

$$\bar{T}_n(\xi, \eta) = t_{\mathrm{ef}} K_0(\xi) K_0(\eta), \tag{15}$$

where the effective global transmittance is given by

$$t_{\mathrm{ef}} = \frac{\prod_{j=1}^{n} t_j}{\prod_{j=1}^{n} (1 - r_j r_{j+1}^*)} \tag{16}$$

with all parameters defined in the theory for a single layer. Note that we have used here the equality: $t_{\mathrm{d}j} = t_j K_0(\xi)$, where $K_0(\xi)$ is the escape function (see Appendix A).

Let us check the applicability of our assumptions making comparisons with exact radiative transfer calculations using SCIATRAN [3] for a special case of a two-layered medium over a black surface. Then Eq. (15) reduces to the following form:

$$\bar{T}_2(\xi, \eta) = \frac{t_1 t_2 K_0(\xi) K_0(\eta)}{1 - r_1 r_2}, \tag{17}$$

where we accounted for the fact that $t_{\mathrm{ef}} = t_1 t_2 (1 - r_1 r_2)^{-1}$ in this case. Note that if both layers do not absorb radiation, then the sensitivity of transmitted light to the vertical inhomogeneity is low

and in a good approximation one can use the reflection function for a single layer having the optical thickness equal to the sum of optical thicknesses of both layers and the average value of the asymmetry parameter to find the solution of the problem at hand [12].

The results of calculations using simple approximation (17) are shown in Figs. 7–9 as functions of the observation angle together with correspondent errors and outcome of exact calculations for the incident angle equal to 60° and the azimuth equal to 0°. In particular, we give the dependence of the transmission function on the observation angle for a single layer having the optical equal to 40 at $\omega_0 = 0.9945$ and 1.0 in Fig. 7a. The results of computations for a two-layered medium having the total optical thickness 40 but $\omega_0 = 0.9945$ in the bottom layer ($\tau_b = 30$) and $\omega_0 = 1.0$ in upper layer ($\tau_u = 10$) are also given in the same figure (the middle line). Note that phase functions in all calculations given here are very close to each other as specified above. So the change of transmission is mostly due to the absorption effect. As expected the largest transmission is observed for a nonabsorbing single layer. It is considerably reduced if absorption is introduced in the bottom part of a layer. Of course, the minimum of transmission occurs for a single absorbing layer (see, e.g. a lower line in Fig. 7a). It follows that exact and approximate results are quite close to each other for observation angles smaller than 70°. Then the error of approximation is smaller than 5% (see Fig. 7c). The error increases for slabs having larger absorption, however. This is illustrated in Fig. 7b, where we show the dependence similar to that in Fig. 7a but for the increased absorption ($\omega_0 = 0.9892$). It is interesting that the error of Eq. (17) for a two-layered medium is smaller than that for a single layer with the optical thickness 40 and $\omega_0 = 0.9892$. This points to the fact that the accuracy of our technique is mostly influenced by the total light absorption and transmission and not by a number of layers (see also Fig. 7c). Note that the accuracy of reflected light calculation is generally higher than that for the diffusely transmitted light (for a given level of absorption).

Calculations for a two-layered turbid slab with the optical thickness of a lower absorbing layer equal to 30 for various thicknesses of a nonabsorbing upper layer $\tau_u = 5, 10, 30$ are shown in Fig. 8a. The middle lines in this figure coincides with the middle line in Fig. 7a. We see that the accuracy is better than 5% in this case. The decrease of the optical thickness of an upper layer leads to the increase of the light transmission as one might expect.

Fig. 8b is similar to 8a, but now the optical thickness of an absorbing layer at the bottom is varied from 5 to 30. The optical thickness of an upper layer is fixed and equal to 10. Clearly, the error approximation increases for thinner layers, which is in accordance with general assumptions of our approximation, which is valid only for weakly absorbing optically thick layers [15]. However Eq. (17) has comparatively high accuracy even at such small values of τ as 5 (see Fig. 8c).

In conclusion, we show the transmission function of a single absorbing layer having optical thickness 40 at $\omega_0 = 0.9945$ in Fig. 9a (middle line) in comparison with transmission functions of a two-layered system having $\omega_0 = 0.9945$ in the upper layer ($\tau_u = 30$) and $\omega_0 = 0.9892$ in the layer at the bottom ($\tau_b = 10$) (lower line in Fig. 9a). Clearly, the transmission for the latter case should be lower. Fig. 9a quantifies this decrease. Upper line in Fig. 9a corresponds to a two-layered system with total optical thickness equal to 40 and local optical characteristics of a lower layer equal to that of a single layer shown by the middle line in Fig. 9a but having a nonabsorbing scattering layer at the top of system ($\tau_u = 10$). Then due to the general decrease of absorption in the system, transmission should increase. This is confirmed by Fig. 9a. It follows from Fig. 9b

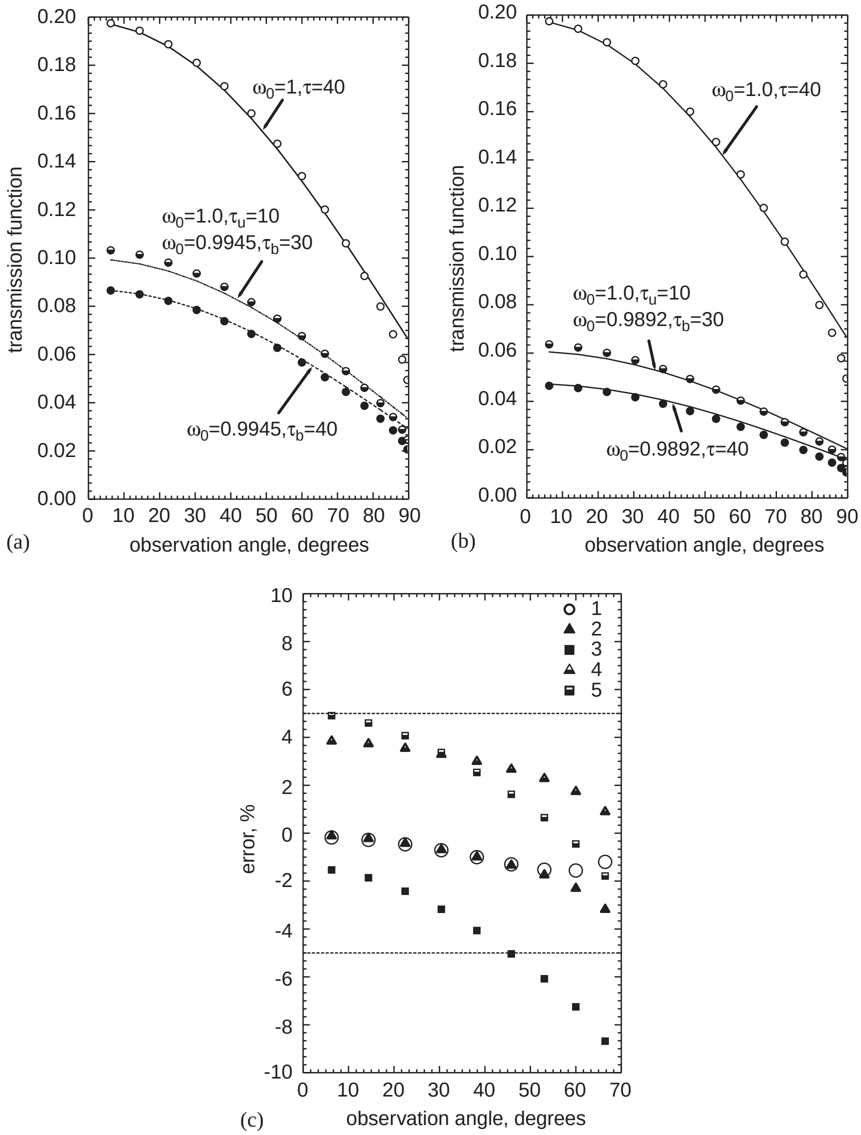

Fig. 7. (a) The dependence of the transmission function on the zenith observation angle at the zenith incidence angle equal to 60° and the azimuth equal to 0° for a single homogeneous layer and a two-layered turbid medium with the total optical thickness equal to 40. The single scattering albedo is equal to 0.9945. Lines correspond to Eq. (17) and symbols are obtained from exact calculations. Further explanations are given in text. (b) The same as in (a) but at $\omega_0 = 0.9892$. (c) Errors of approximation (17) for cases considered in (a) and (b) (1, 2, 3—single layers with the optical thickness 40 and $\omega_0 = 1.0$, 0.9945 and 0.9892, respectively; 4,5—two-layered systems with a nonabsorbing top layer having optical thickness 10 and an absorbing layer at bottom with $\omega_0 = 0.9945$ (4), $\omega_0 = 0.9892$ (5)).

that the error of Eq. (17) is smaller than 5%, which is acceptable for a broad range of applications (e.g., rapid estimations of stratification effects on diffusely transmitted and reflected light fields).

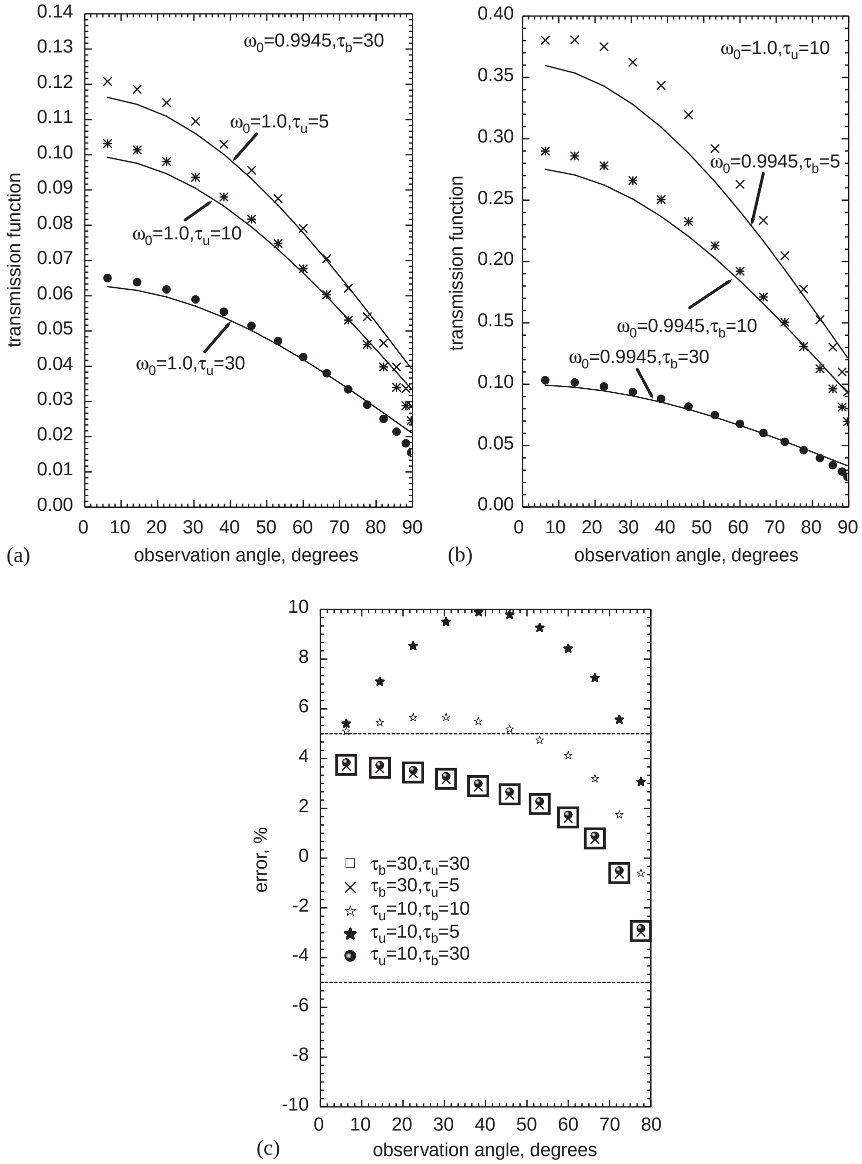

Fig. 8. (a) The same as in Fig. 7a but for other values of optical thickness of an upper layer. (b) The same as in Fig. 7a but for other values of optical thickness of a bottom layer. (c) The error of approximation given by Eq. (17).

3. Conclusion

We derived here simple analytical equations for reflection and transmission functions of multi-layered turbid media in the assumption that each layer is optically thick ($\tau > 5$) and weakly absorbing ($\beta \leqslant 0.03$). They can be used to solve a variety of practical problems including light

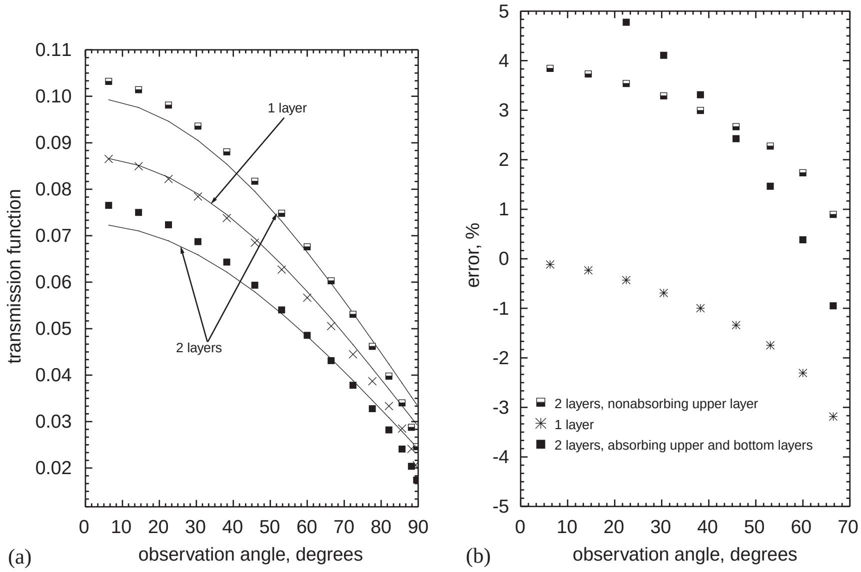

Fig. 9. (a) The dependence of the transmission function on the zenith observation angle at the zenith incidence angle equal to 60° and the azimuth equal to 0° for a single homogeneous layer (middle line, $\omega_0 = 0.9945$, $\tau = 40$) and a two-layered turbid medium ($\omega_0 = 0.9945$, $\tau = 30$ for a lower layer and $\omega_0 = 1.0$, $\tau = 10$ for an upper layer (upper line) and $\omega_0 = 0.9892$, $\tau = 10$ for a lower layer and $\omega_0 = 0.9945$, $\tau = 30$ for an upper layer (lower line)). Lines correspond to results obtained with Eq. (17) and symbols are obtained from exact calculations. Further explanations are given in text. (b) Errors of Eq. (17) correspondent to data given (a).

propagation in stratified snow and clouds. The error of equations for the cases studied here is below 15% (for most of geometries the error is below 5%).

Note that equations presented above should be used only in the case of absorbing layers. For nonabsorbing layers the sensitivity of reflection and transmission to the stratification is low. Then the theory of a single layer with an averaged asymmetry parameter and integral optical thickness equal to the sum of optical thicknesses of all layers should be preferably used.

Acknowledgements

This work was supported by the DFG Project BU 688/8-1.

Appendix A

Here we present in a condensed form main equations for a single scattering layer proposed by Kokhanovsky and Rozanov [8]. Namely, it follows:

$$R(\xi, \eta, \tau) = R_\infty(\xi, \eta) - T(\xi, \eta, \tau)\exp(-x - y),$$

where

$$R_\infty(\xi,\eta,\phi) = R^0_\infty(\xi,\eta,\phi)\exp(-(1-0.05y)u),$$

$$T(\tau,\xi,\eta) = \left(\frac{sh(y)}{sh(x+\alpha y)} - t_c\exp(x)\right)K_0(\xi)K_0(\eta),$$

$$K_0(\xi) = \frac{3}{7}(1+2\xi), \quad t_c = \frac{a - b\xi\eta + c\eta^2\xi^2}{\tau^3}, \quad u = \frac{K_0(\xi)K_0(\eta)}{R^0_\infty(\xi,\eta,\phi)},$$

$$x = \sqrt{3(1-g)\beta}\tau, \quad y = 4\sqrt{\frac{\beta}{3(1-g)}},$$

$a = 4.86$, $b = 13.08$, $c = 12.76$, β is the probability of photon absorption and g is the asymmetry parameter, ξ and η are cosines of incident and observation zenith angles, respectively, ϕ is the azimuth. The function $R^0_\infty(\xi,\eta,\phi)$ gives the reflection function for a semi-infinite nonabsorbing medium. It only weakly depends on the size of particles but considerably depends on their shape (see Fig. A1). We used the following parameterizations for this functions valid for the nadir observation geometry:

$$R^0_\infty(\xi,1) = \frac{0.37+1.94\xi}{1+\xi} + \frac{p(\pi - \arccos\xi)}{4(1+\xi)}$$

for water clouds and

$$R^0_\infty(\xi,1) = 0.61284\xi + 0.8\xi - 0.33849\xi^2$$

for ice clouds. The accuracy of these approximations is quite high as follows from Fig. A.1. Results in Fig. A.1 are obtained for the gamma size distribution of water droplets $f(a) = Ba^6\exp(-9a/a_{\mathrm{ef}})$, $B = \mathrm{const}$, a is the radius of droplets. The phase function of ice particles was taken from data given by Mishchenko et al. [14] for a fractal ice particle. The wavelength is equal to 0.65 μm.

The equation for the function $R^0_\infty(\xi,\eta,\phi)$ for other observation conditions is given by Kokhanovsky [16]. The phase function $p(\theta)$ can be calculated using Mie theory. However, we used here the following approximate expression valid for water clouds [17]:

$$p(\theta) = n\mathrm{e}^{-v\theta} + \sum_{i=1}^{5}\gamma_i \mathrm{e}^{-\delta_i(\theta-\theta_i)^2},$$

where θ is the scattering angle in radians, $n = 17.7$, $v = 3.9$ and constants γ_i, δ_i, θ_i are presented in Table A.1.

The reflection and transmission functions given above can be used to calculate various other radiative characteristics including the diffuse transmittance $t_{\mathrm{d}}(\xi)$, the global transmittance t, the plane albedo $\Re(\xi)$, and the spherical albedo r. Correspondent equations are given in Table A.2. Note that to derive formulae in Table A.2 from equations given above we neglected a small term

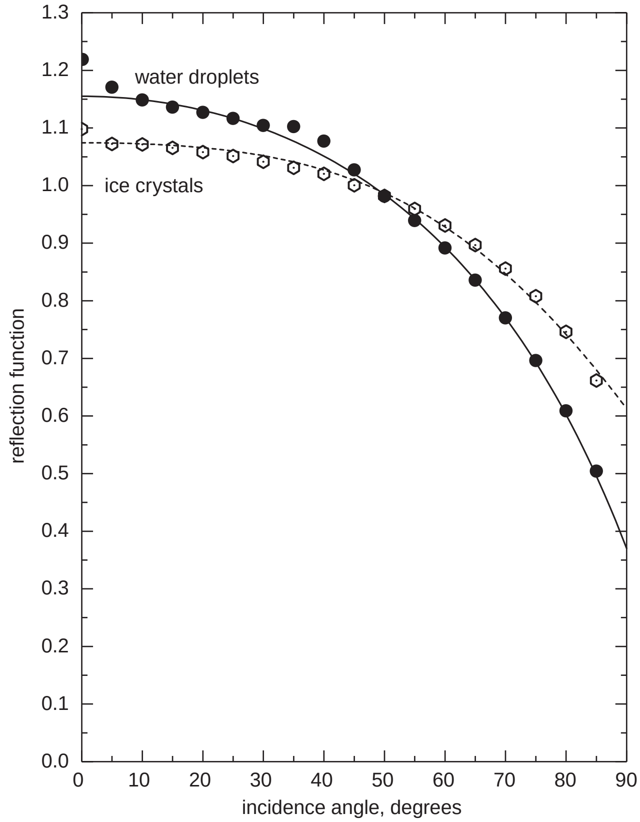

Fig. A.1. The dependence of reflection functions of a semi-infinite nonabsorbing water and ice cloud on the incidence angle at the nadir observation. Symbols give exact results and lines are due to the approximation (see details in text).

Table A.1
Parameters γ_i, δ_i, and θ_i [18]

i	γ_i	δ_i	θ_i
1	1744.0	1200.0	0.0
2	0.17	75.0	2.5
3	0.30	4826.0	π
4	0.20	50.0	π
5	0.15	1.0	π

$t_c \sim \tau^{-3}$. Also we used the equality

$$2\int_0^1 K_0(\xi)\xi\,\mathrm{d}\xi = 1$$

and approximate integration techniques described by Kokhanovsky [17].

Table A.2
Radiative characteristics of optically thick weakly absorbing strongly light scattering turbid layers [17]

Radiative characteristic	Symbol	Definition	Equation
Plane albedo	$\Re(\xi)$	$2\int_0^1 R(\xi,\eta)\eta\,d\eta$	$\Re_\infty(\xi) - (r_\infty - r)K_0(\xi)$
Spherical albedo	r	$2\int_0^1 \Re(\xi)\xi\,d\xi$	$r_\infty - t\exp(-x-y)$
Diffused transmittance	$t_d(\xi)$	$2\int_0^1 \mathrm{T}(\xi,\eta)\eta\,d\eta$	$tK_0(\xi)$
Global transmittance	t	$2\int_0^1 t_d(\xi)\xi\,d\xi$	$\frac{\sinh(y)}{\sinh(x+\alpha y)}$

Functions given in table are defined using following equations:

$$R \equiv \frac{1}{2\pi}\int_0^{2\pi} R(\xi,\eta,\phi)\,d\phi, \quad \mathrm{T} \equiv \frac{1}{2\pi}\int_0^{2\pi} T(\xi,\eta,\phi)\,d\phi,$$

$$\Re_\infty(\xi) = \exp[-y(1-0.05y)K_0(\xi)], \quad K_0(\xi) = \frac{3}{7}(1+2\xi),$$

$$r_\infty = e^{-y}, \quad x = k\tau, \quad y = k\tau, \quad k = \sqrt{3(1-\omega_0)(1-g)}, \quad \alpha = 1.07.$$

The light absorptance by the disperse medium under consideration for the mono-directional illumination $A(\xi)$ and for the diffuse illumination a can be also derived. Namely, it follows using the energy conservation law: $A(\xi) = 1 - t_d(\xi) - \Re(\xi)$ and $a = 1 - r - t$.

References

[1] Yanovitskij EG. Light scattering in inhomogeneous atmospheres. New York: Springer; 1997.
[2] Minin IN. Radiative transfer theory in planetary atmospheres. Moscow: Nauka; 1988.
[3] Rozanov VV, et al. SCIATRAN—a new radiative transfer model for geophysical applications in the 240–2400 nm spectral range: the pseudo-spherical version. Adv Space Res 2002;29:1831–5.
[4] Germogenova TA, Konovalov NV. Asymptotic characteristic solutions of transport equation for the inhomogeneous slab problem. J Appl Math Comput Phys 1974;14:928–46.
[5] Ivanov VV. Radiative transfer in multi-layered optically thick atmosphere. Part I. Trans Astron Obs LGU 1976;32:3–23.
[6] Ivanov VV. Radiative transfer in multi-layered optically thick atmosphere. Part II. Trans Astron Obs LGU 1976;32:23–39.
[7] Vasilyev AB, Melnikova IN. Short-wave solar radiation in the Earth's atmosphere. Calculations. Observations. Interpretation. St. Petersburg: St. Petersburg University Publishing House; 2002.
[8] Kokhanovsky AA, Rozanov VV. The physical parameterization of the top-of-atmosphere reflection function for a cloudy atmosphere—underlying surface system: the oxygen A-band case study. JQSRT 2004;85:35–55.
[9] Rozenberg GV. Optical characteristics of thick weakly absorbing scattering layers. Doklady AN SSSR 1962;145:775–7.
[10] Melnikova IN, Minin IN. On the monochromatic radiative transfer in cloud layers. Izv Atmos Ocean Phys 1997;13(3):254–63.
[11] Zege EP, Ivanov AP, Katsev IL. Image transfer through a scattering medium. New York: Springer; 1991.
[12] Sobolev VV. Light scattering in planetary atmospheres. Moscow: Nauka; 1972.
[13] Kokhanovsky AA. Light scattering media optics: problems and solutions. Berlin: Springer-Praxis; 2002.

[14] Mishchenko MI, Dlugach JM, Yanovitskij EG, Zakharova NT. Bidirectional reflectance of flat, optically thick particulate layers: an efficient radiative transfer solution and applications to snow and soil surfaces. JQSRT 1999;63:409–32.
[15] Kokhanovsky AA, Rozanov VV. The reflection function of optically thick weakly absorbing turbid layers: a simple approximation. JQSRT 2003;77:165–75.
[16] Kokhanovsky AA. Reflection of light from nonabsorbing semi-infinite cloudy media: a simple approximation. JQSRT 2004;85:35–55.
[17] Kokhanovsky AA, et al. A semi-analytical cloud retrieval algorithm using backscattered radiation in 0.4–2.4 micrometers spectral range. J Geophys Res D 2003;108:D1 10.1029/2001JD001543.
[18] Kokhanovsky AA. Optical properties of semi-infinite turbid media: some simple approximations. Opt Eng 2003;42:2040–6.